

Predicting treatment outcomes using ¹⁸F-FDG PET biomarkers in patients with non-small-cell lung cancer receiving chemoimmunotherapy

Chang Gon Kim*, Sang Hyun Hwang*, Kyung Hwan Kim, Hong In Yoon, Hyo Sup Shim, Ji Hyun Lee, Yejeong Han, Beung-Chul Ahn, Min Hee Hong, Hye Ryun Kim, Byoung Chul Cho, Arthur Cho and Sun Min Lim

Ther Adv Med Oncol

2022, Vol. 14: 1–13

DOI: 10.1177/
17588359211068732

© The Author(s), 2022.
Article reuse guidelines:
sagepub.com/journals-
permissions

Abstract

Background: Predictive markers for treatment response and survival outcome have not been identified in patients with advanced non-small-cell lung cancer (NSCLC) receiving chemoimmunotherapy. We aimed to evaluate whether imaging biomarkers of ¹⁸F-fluorodeoxyglucose (¹⁸F-FDG) positron emission tomography/computed tomography (PET/CT) and routinely assessed clinico-laboratory values were associated with clinical outcomes in patients with advanced NSCLC receiving pembrolizumab plus platinum-doublet chemotherapy as a first-line treatment.

Methods: We retrospectively enrolled 52 patients with advanced NSCLC who underwent baseline ¹⁸F-FDG PET/CT before treatment initiation. PET/CT parameters and clinico-laboratory variables, constituting the prognostic immunotherapy scoring system, were collected. Optimal cut-off values for PET/CT parameters were determined using the maximized log-rank test for progression-free survival (PFS). A multivariate prediction model was developed based on Cox models for PFS, and a scoring system was established based on hazard ratios of the predictive factors.

Results: During the median follow-up period of 16.7 months (95% confidence interval: 15.7–17.7 months), 43 (82.7%) and 31 (59.6%) patients experienced disease progression and death, respectively. Objective response was observed in 23 (44.2%) patients. In the multivariate analysis, maximum standardized uptake value, metabolic tumour volume_{2.5}, total lesion glycolysis_{2.5}, and bone marrow-to-liver uptake ratio from the PET/CT variables and neutrophil-to-lymphocyte ratio (NLR) from the clinico-laboratory variables were independently associated with PFS. The scoring system based on these independent predictive variables significantly predicted the treatment response, PFS, and overall survival.

Conclusion: PET/CT variables and NLR were useful biomarkers for predicting outcomes of patients with NSCLC receiving pembrolizumab and chemotherapy as a first-line treatment, suggesting their potential as effective markers for combined PD-1 blockade and chemotherapy.

Keywords: ¹⁸F-FDG PET/CT, chemoimmunotherapy, non-small-cell lung cancer, predictive model, treatment outcome

Received: 3 September 2021; revised manuscript accepted: 2 December 2021.

Introduction

Antibodies targeting immune checkpoint co-inhibitory receptors have revolutionized the treatment

landscape of non-small-cell lung cancer (NSCLC), and the use of immune checkpoint blockade (ICB) has become the mainstay treatment strategy for

Correspondence to:

Arthur Cho
Department of Nuclear
Medicine, Severance
Hospital, Yonsei University
College of Medicine, 50-1
Yonsei-ro, Seodaemun-gu,
Seoul 03722, Republic of
Korea.

artycho@yuhs.ac

Sun Min Lim
Division of Medical
Oncology, Department of
Internal Medicine, Yonsei
Cancer Centre, Yonsei
University College of
Medicine, 50-1 Yonsei-ro,
Seodaemun-gu, Seoul
03722, Republic of Korea.
limlove2008@yuhs.ac

Chang Gon Kim
Ji Hyun Lee
Yejeong Han
Beung-Chul Ahn
Min Hee Hong
Hye Ryun Kim
Byoung Chul Cho
Division of Medical
Oncology, Department of
Internal Medicine, Yonsei
Cancer Centre, Yonsei
University College of
Medicine, Seoul, Republic
of Korea

Sang Hyun Hwang
Department of Nuclear
Medicine, Severance
Hospital, Yonsei University
College of Medicine, Seoul,
Republic of Korea

Kyung Hwan Kim
Hong In Yoon
Department of Radiation
Oncology, Yonsei Cancer
Centre, Yonsei University
College of Medicine, Seoul,
Republic of Korea

Hyo Sup Shim
Department of Pathology,
Severance Hospital, Yonsei
University College of
Medicine, Seoul, Republic
of Korea

*Joint first authors.

NSCLC.¹⁻³ Among various PD-1 inhibitors, pembrolizumab and nivolumab have been shown to significantly prolong the survival in patients with advanced NSCLC.⁴⁻¹⁰ Importantly, treatment response in the case of PD-1 blockade as a single agent is moderate and enriched in specific patient populations.¹¹ For example, PD-L1 expression,^{12,13} spatial and temporal distribution of tumour-infiltrating lymphocytes,¹⁴ tumour mutation burden,¹⁵ gene expression profiles,¹⁶ and human leucocyte antigen heterogeneity¹⁷ have been suggested as biomarkers to predict the treatment outcomes as a single agent.¹⁸ To enhance the therapeutic benefits and survival outcomes, of PD-1 inhibitors as a monotherapy,¹⁹⁻²¹ combining PD-1 blockade with chemotherapy has been explored as a therapeutic modality and has successfully demonstrated superiority in both nonsquamous and squamous histologies.^{6,10} Based on the results of these pivotal studies, a combination of pembrolizumab and chemotherapy is recommended as a first-line treatment in patients with NSCLC without oncogenic alterations. However, there are no predictive markers that can stratify patients into subgroups who would derive clinical benefits from treatment with such a combined chemoimmunotherapeutic approach.

Measurement of glycolysis in tumours and other organs by ¹⁸F-fluorodeoxyglucose (¹⁸F-FDG) positron emission tomography/computed tomography (PET/CT) is useful in predicting outcomes in patients receiving ICB.²² For instance, ¹⁸F-FDG PET/CT has proven its predictive value in patients receiving ICB^{23,24} or chemotherapy in NSCLC.^{25,26} In several recent studies, ¹⁸F-FDG uptake of lymphoid cell-rich organs, such as the spleen or bone marrow, had predictive value for clinical outcome in solid tumours including NSCLC.²⁷⁻³⁰

Furthermore, systemic inflammatory processes can exert a deleterious effect on prognosis through interaction with tumour microenvironment and promote tumour growth via modulating the concentration of proinflammatory cytokines (IL-1 β and IL-6) and abundance of the myeloid-derived suppressor cells.³¹ However, whether the PET/CT-related variables and index for systemic inflammation have predictive roles in patients with NSCLC who are treated with chemoimmunotherapy has not yet been addressed.

Given the extensive heterogeneous nature and systemic alterations in glycolysis induced by NSCLC, we explored whether comprehensive assessment of variables derived from ¹⁸F-FDG

PET/CT could significantly predict outcomes in individual patients during treatment with chemoimmunotherapy. In addition, we selected various previously known predictive factors for treatment responses and immunotherapy outcomes to investigate the independent predictive value of the PET/CT-related variables. Finally, we conceived a model to predict the outcomes of patients with NSCLC treated with chemoimmunotherapy, which has not been attempted before.

Materials and methods

Patients

We retrospectively enrolled 71 patients with advanced NSCLC who were treated with an anti-PD-1 antibody (pembrolizumab) combined with platinum-based chemotherapy as a first-line treatment between September 2017 and September 2020. Patients with either nonsquamous or squamous histology who were treated with pembrolizumab plus chemotherapy as a first-line treatment were eligible, based on which, we included 52 patients for the subsequent analyses. Patients with an undetermined histology ($n = 1$) and those who received combination chemoimmunotherapy as a second or higher line of treatment ($n = 18$) were excluded. All enrolled patients underwent ¹⁸F-FDG PET/CT before treatment. The Institutional Review Board of Yonsei University College of Medicine approved this study (IRB approved no. 4-2021-0358). The Institutional Review Board waived the need for informed consent from the patients enrolled in this study based on its retrospective nature.

¹⁸F-FDG PET/CT imaging

All patients fasted for at least 6 h before the PET/CT study. Blood glucose levels were measured and were required to be less than 140 mg/dl. Whole-body PET and unenhanced CT images were acquired using a PET/CT scanner (Discovery 710, 600; General Electric Medical Systems, Milwaukee, WI, USA). Briefly, 3.7 MBq/kg of ¹⁸F-FDG was intravenously injected 60 min before the imaging. After an initial low-dose CT (tube voltage, 120 kV; tube current, auto mA), a PET scan was obtained, extending from the skull base to the proximal thighs, with an acquisition time of 2 min per bed position in a three-dimensional mode. PET images were reconstructed using ordered-subset expectation maximization (two iterations, 16 subsets).

Image analysis

¹⁸F-FDG PET/CT images were reviewed by two nuclear medicine physicians using a commercial software (MIM 6.9.7; MIM Software Inc., Cleveland, OH, USA). All primary and metastatic lesions were selected for analysis, and maximum standardized uptake value (SUV_{max}), SUV_{mean}, metabolic tumour volume (MTV), and total lesion glycolysis (TLG) of each lesion were automatically measured by the analysis software. The SUV of the volume of interest was calculated as follows: [decay-corrected activity (kBq) volume (ml) dose (kBq) weight (g)].

MTV was defined as total volume with an SUV of 2.5 or greater (MTV_{2.5}) or up to 41% of SUV_{max} (MTV_{41%}). The TLG was calculated by multiplying mean SUV by MTV_{2.5} or MTV_{41%} inside the tumour boundaries and named as follows: TLG_{2.5} and TLG_{41%}. A threshold of 2.5 SUV had shown good predictive values for patients with NSCLC in most studies,³² and 41% SUV_{max} was recommended by the European Association of Nuclear Medicine,³³ so both thresholds were used in the present study. The SUV_{max} of each patient was defined as the highest SUV_{max} among all lesions detected in that patient. Total MTV and total TLG were defined as the sum of the MTV and TLG of all lesions, respectively. Normal liver activity was measured by drawing three spheric 1 cm regions of interest (ROI) on the normal liver: two on the right lobe and one on the left lobe. The SUV_{mean} of the liver was defined as the mean of these three mean SUVs of ROIs. Spleen SUV_{mean} was obtained from 1 cm ROI on three nonadjacent slices and then we averaged these three mean SUV of ROIs. Bone marrow SUV_{mean} was obtained by drawing ROIs over the centre of each 1–5 lumbar vertebrae unless a pathologic lesion such as bone metastasis, compression fracture, or undergoing operation for spinal disease was present, and then averaging the mean SUV of ROIs. The spleen-to-liver ratio of SUV (SLR) was calculated by dividing the spleen SUV_{mean} by the liver SUV_{mean}, and the bone marrow-to-liver ratio of the SUV (BLR) was calculated by dividing the bone marrow SUV_{mean} by the liver SUV_{mean}, similarly to previous reports.^{28–30,34,35}

Follow-up and response evaluation

Laboratory tests and physical examinations were performed at every cycle of administration with an anti-PD-1 antibody and chemotherapy.

Treatment response was evaluated *via* imaging analysis, including CT and magnetic resonance imaging. Tumour imaging was performed at weeks 6 and 12, every 9 weeks until week 48, and every 12 weeks after then. Based on the Response Evaluation Criteria in Solid Tumours version (RECIST) 1.1, treatment response was classified as complete response, partial response, stable disease, or progressive disease.³⁶ The cut-off date of data was 31 October 2021. During the study period, four patients were lost follow-up and were censored at the last date of known survival status.

Statistical analysis

Variables for survival analyses included age, sex, smoking, histology, PD-L1 tumour proportion score (TPS), and PET/CT parameters. In addition, variables previously known to be related with immunotherapy outcomes were also analysed. These factors included the albumin level, lactate dehydrogenase (LDH) level, number of metastatic sites, neutrophil-to-lymphocyte ratio (NLR), or derived NLR [dNLR; calculated as neutrophil count/(leucocyte count – neutrophil count)], all of which constituted the predictive scoring system for immunotherapy.^{37–39} For the statistical analyses, PET/CT parameters were dichotomized into two categories using maximal log-rank test for determining the progression-free survival (PFS), since there are no definite cut-off values for PET/CT parameters for predicting the survival of patients with NSCLC. PFS was measured as the time from the initiation of treatment to disease progression or death. Overall survival (OS) was measured as the time from the initiation of treatment to death from any cause. Survival curves were plotted using the Kaplan–Meier method, and differences between subgroups were compared using the log-rank test. Cox proportional hazards model was used for the univariate and multivariate analyses. Factors significantly associated with PFS in the multivariate analysis based on a stepwise approach were selected for constructing a nomogram, and the weighted risk score of each variable in the model was calculated based on β -regression coefficient by the Cox-regression model. Based on the total points, patients were categorized into four risk subgroups: low, intermediate-low, intermediate-high, and high. Differences among the continuous and categorical variables were examined for significance as per Student's *t* test and chi-squared test. All statistical analyses were performed using

R version 4.0.4 (<http://www.R-project.org>) and GraphPad Prism version 6.0 (GraphPad Software, San Diego, CA); p values <0.05 were considered significant.

Results

Patient characteristics

Total 52 patients were included in the final analysis (Table 1). The median age of the patients was 63 years, and majority of them were men (41/52, 78.8%) and smokers (36/52, 69.2%). Nonsquamous carcinoma histology was more common (39/52, 75.0%) than squamous carcinoma histology (13/52, 25.0%). PD-L1 TPS was 0% in 21 (40.4%), 1–49% in 19 (36.5%), and $\geq 50\%$ in 12 (23.1%) patients, respectively. No patients harboured tumours with oncogenic alterations, including *EGFR* mutation, *ALK* rearrangement, and *ROS1* rearrangement. Pembrolizumab, pemetrexed, and carboplatin were administered to patients with a nonsquamous histology, whereas pembrolizumab, paclitaxel, and carboplatin were administered to patients with a squamous histology. Objective response and disease control were achieved in 23 (44.2%) and 42 patients (80.8%), respectively. During the median follow-up period of 16.7 months [95% confidence interval (CI): 15.7–17.7 months], median PFS and OS were 6.4 months (95% CI: 1.3–11.4 months) and 15.0 months (95% CI: 6.8–23.2 months), respectively. There were no differences in the response and survival outcomes according to age, sex, smoking status, histologic subtypes, PD-L1 expression, and the prescribed regimen (Supplemental Table 1; Supplemental Figure 1).

Survival outcome according to the PET-derived index and immunotherapy-related index

Next, we assessed whether PET/CT biomarkers and known factors associated with immunotherapy outcomes were predictive markers for the survival outcomes. ^{18}F -FDG PET/CT was performed before the initiation of treatment, and the interval between the ^{18}F -FDG PET/CT scan and the first treatment was a median of 13 days (range: 0–56 days). To assess the predictive significance of the PET/CT biomarkers, cut-offs for each PET/CT variable were identified by log-rank maximization method for PFS (Supplemental Table 2). Cut-off for immunotherapy-related variables was set as per the previously suggested value (Supplemental Table 2).^{37–39} All selected PET/CT variables,

including SUVmax, MTV, TLG, SLR, and BLR, were significantly associated with both PFS and OS (Figure 1). Among the previously suggested clinical and laboratory variables for predicting the immunotherapy outcomes, the baseline albumin level and dNLR were not significantly associated with the survival outcomes in both PFS and OS, whereas the sites of metastasis, LDH, and NLR were significantly associated with both PFS and OS (Figure 2).

Next, we investigated whether each variable was independently associated with PFS via multivariate analysis in a stepwise manner (Supplemental Figure 2). Since there was an intrinsically significant correlation between $\text{MTV}_{2.5}$ versus $\text{MTV}_{41\%}$, $\text{TLG}_{2.5}$ versus $\text{TLG}_{41\%}$, and SLR versus BLR , we compared the predictive value of each pair of variables (Table 2). The analysis revealed that $\text{MTV}_{2.5}$, $\text{TLG}_{2.5}$, and BLR were superior than other variables in terms of PFS predictive value, prompting us to conduct subsequent analyses with these variables. In addition, patient subgroups classified on the basis of $\text{MTV}_{2.5}$ and $\text{TLG}_{2.5}$ values were completely overlapping, prompting us to conduct multivariate analysis with PET/CT variables with SUVmax, $\text{MTV}_{2.5}$ ($\text{TLG}_{2.5}$), and BLR , which were significantly related to PFS. Among the clinicolaboratory variables, only NLR was significantly associated with PFS in the multivariate analysis. Final multivariate analysis, encompassing SUVmax, $\text{MTV}_{2.5}$ ($\text{TLG}_{2.5}$), BLR , and NLR, confirmed that these variables could independently predict the PFS (Supplemental Table 3). In the analysis for OS, similar results were obtained (Supplemental Table 4). Collectively, the ^{18}F -FDG PET/CT index, including SUVmax, MTV, TLG, and BLR, could successfully predict the outcome of chemoimmunotherapy, whereas only NLR was associated with the outcome of chemoimmunotherapy among the clinicolaboratory variables.

Establishment of a predictive model for the chemoimmunotherapeutic outcomes

Next, we constructed a model for predicting the outcomes, which comprised factors that were independently associated with PFS in the multivariate analysis (Figure 3(a)). This scoring model system yielded four patient subgroups (low, intermediate-low, intermediate-high, and high) based on the summation of the risk scores (Figure 3(b)). Treatment response was substantially different according to the different risk subgroups (Figure

3(c)), suggesting that this classification was predictive rather than prognostic in patients receiving chemoimmunotherapy. Correspondingly, distinct survival outcomes were observed both in the case of PFS (Figure 3(d)) and OS (Figure 3(e)). Collectively, a predictive model encompassing ^{18}F -FDG PET/CT index and NLR could be used to significantly predict the treatment outcomes in terms of response and survival.

Discussion

Combined chemoimmunotherapy is now considered as the standard treatment modality for advanced NSCLC irrespective of PD-L1 expression.^{40,41} Contrary to other treatment strategies, such as tyrosine kinase inhibitors targeting oncogenic alterations or single-agent PD-1 blockade, predictive markers for combined chemoimmunotherapy have not yet been established. In this study, we comprehensively analysed ^{18}F -FDG PET/CT parameters and clinicolaboratory variables to construct a predictive model for treatment outcomes in patients with NSCLC treated with upfront chemoimmunotherapy. Variables associated with tumour volume (MTV or TLG), tumour glycolysis (SUVmax), and bone marrow glycolysis (BLR) were independently associated with the treatment outcome along with NLR. To the best of our knowledge, this is the first study to suggest predictive biomarkers for chemoimmunotherapy in advanced NSCLC.

The role of ^{18}F -FDG PET/CT in the diagnosis, staging, and follow-up for NSCLC has been well established.⁴⁰ Moreover, predictive or prognostic role of tumour metabolism measured on the basis of ^{18}F -FDG PET/CT has been investigated in patients with NSCLC treated with immunotherapy,^{42,43} chemotherapy,⁴⁴ tyrosine kinase inhibitors,⁴⁵ and concurrent chemo-radiotherapy.⁴⁶ In addition to the glycolytic index of a tumour, ^{18}F -FDG uptake by normal organs, such as the bone marrow, has been suggested to predict the outcomes of patients with NSCLC.⁴⁷ In the current study, we thoroughly evaluated ^{18}F -FDG uptake of tumours as well as normal organs, including spleen and bone marrow, using ^{18}F -FDG PET/CT. By incorporating other predictive variables derived from the immunotherapy scoring system, we found that ^{18}F -FDG PET/CT parameters could independently predict the survival outcome of chemoimmunotherapy, shedding light on the usefulness of ^{18}F -FDG PET/CT in the current treatment protocol for NSCLC for the first time.

Table 1. Patients' characteristics.

	Total patients (n = 52)
Median age, years (range)	63 (33–84)
Sex	
Male	41 (78.8%)
Female	11 (21.2%)
Smoking	
Current	7 (13.5%)
Ex-smoker	29 (55.8%)
Never smoker	16 (30.8%)
Histology	
Nonsquamous	39 (75.0%)
Squamous	13 (25.0%)
PD-L1 TPS	
0%	21 (40.4%)
1–49%	19 (36.5%)
≥50%	12 (23.1%)
Mean PET/CT index (standard deviation)	
SUVmax	14.3 (7.1)
MTV _{41%}	78.8 (80.4)
MTV _{2.5}	188.7 (196)
TLG _{41%}	695.8 (918.2)
TLG _{2.5}	1227.0 (1598.9)
Spleen-to-liver uptake ratio	0.85 (0.15)
Bone marrow-to-liver uptake ratio	0.75 (0.18)
Mean neutrophil-to-lymphocyte ratio (standard deviation)	3.83 (3.37)
Treatment	
Pembrolizumab + pemetrexed + carboplatin or cisplatin	39 (75.0%)
Pembrolizumab + paclitaxel + carboplatin	13 (25.0%)
Best response	
Complete response	1 (1.9%)
Partial response	22 (42.3%)
Stable disease	19 (36.5%)
Progressive disease	10 (19.2%)
MTV, metabolic tumour volume; PD-L1, programmed death ligand-1; PET/CT, positron emission tomography/computed tomography; SUVmax, maximum standardized uptake value; TLG, total lesion glycolysis; TPS, tumour proportion score.	

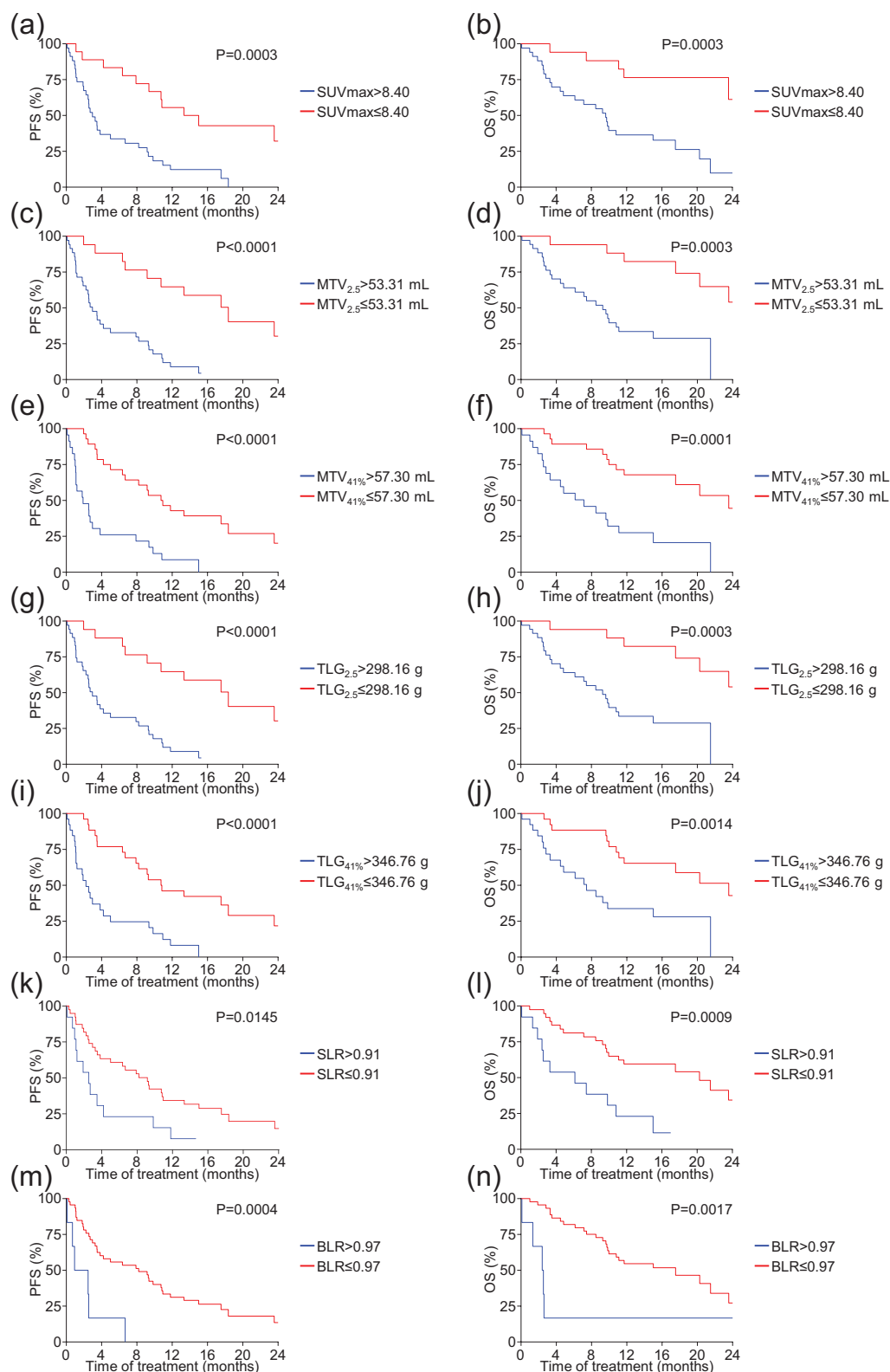


Figure 1. Survival outcomes according to the ^{18}F -FDG PET/CT index. (a) PFS and (b) OS according to SUVmax. (c) PFS and (d) OS according to $\text{MTV}_{2.5}$. (e) PFS and (f) OS according to $\text{MTV}_{41\%}$. (g) PFS and (h) OS according to $\text{TLG}_{2.5}$. (i) PFS and (j) OS according to $\text{TLG}_{41\%}$. (k) PFS and (l) OS according to SLR. (m) PFS and (n) OS according to BLR. ^{18}F -FDG, ^{18}F -fluorodeoxyglucose; MTV, metabolic tumour volume; OS, overall survival; PET/CT, positron emission tomography/computed tomography; PFS, progression-free survival; SUVmax, maximum standardized uptake value; TLG, total lesion glycolysis.

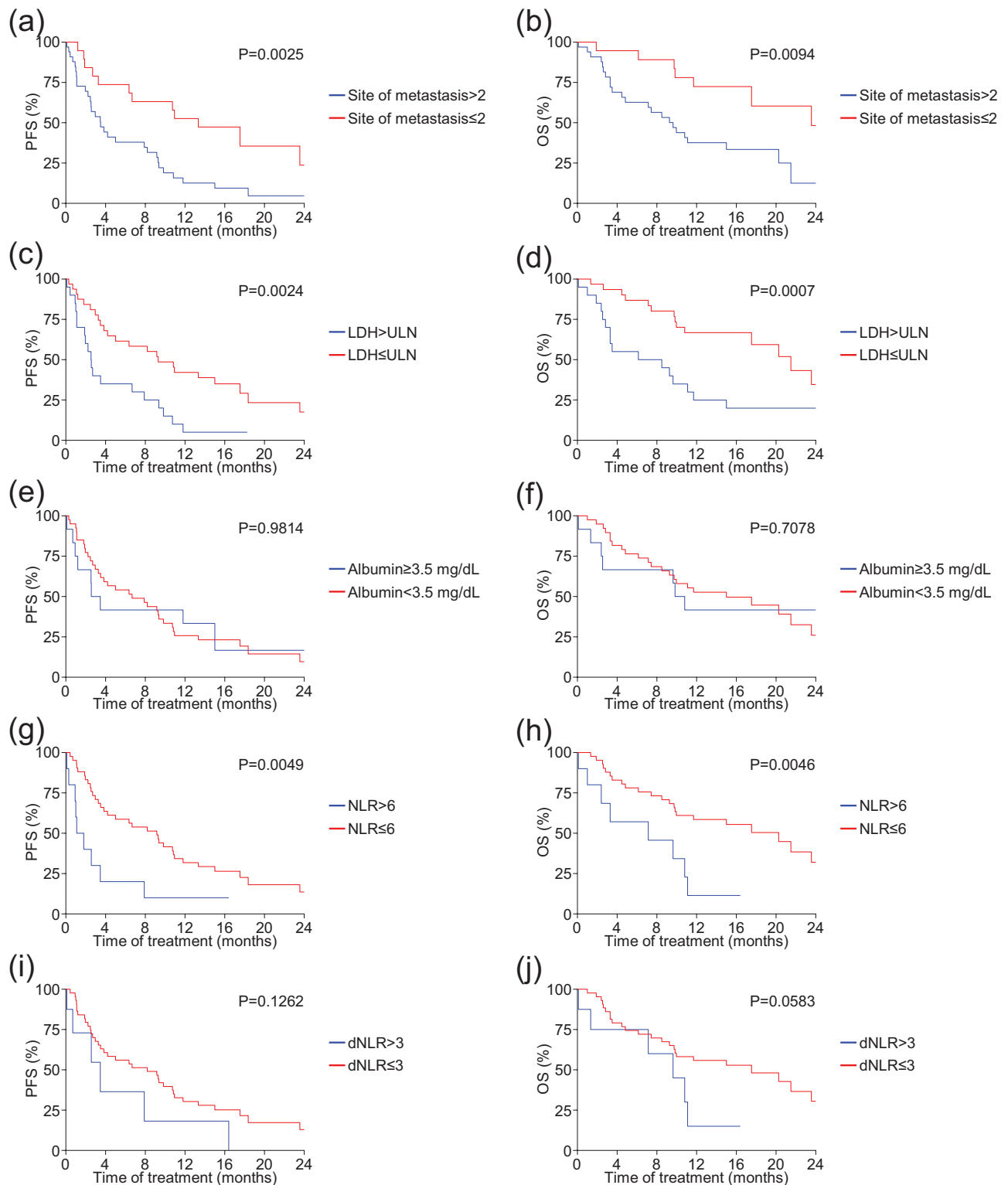


Figure 2. Survival outcomes according to the immunotherapy-related index. (a) PFS and (b) OS according to number of sites of metastasis. (c) PFS and (d) OS according to the baseline LDH level. (e) PFS and (f) OS according to the baseline albumin level. (g) PFS and (h) OS according to the baseline NLR. (i) PFS and (j) OS according to the baseline dNLR. dNLR, derived NLR; LDH, lactate dehydrogenase; NLR, neutrophil-to-lymphocyte ratio; OS, overall survival; PFS, progression-free survival.

Table 2. Univariate and multistep multivariate analysis for progression-free survival.

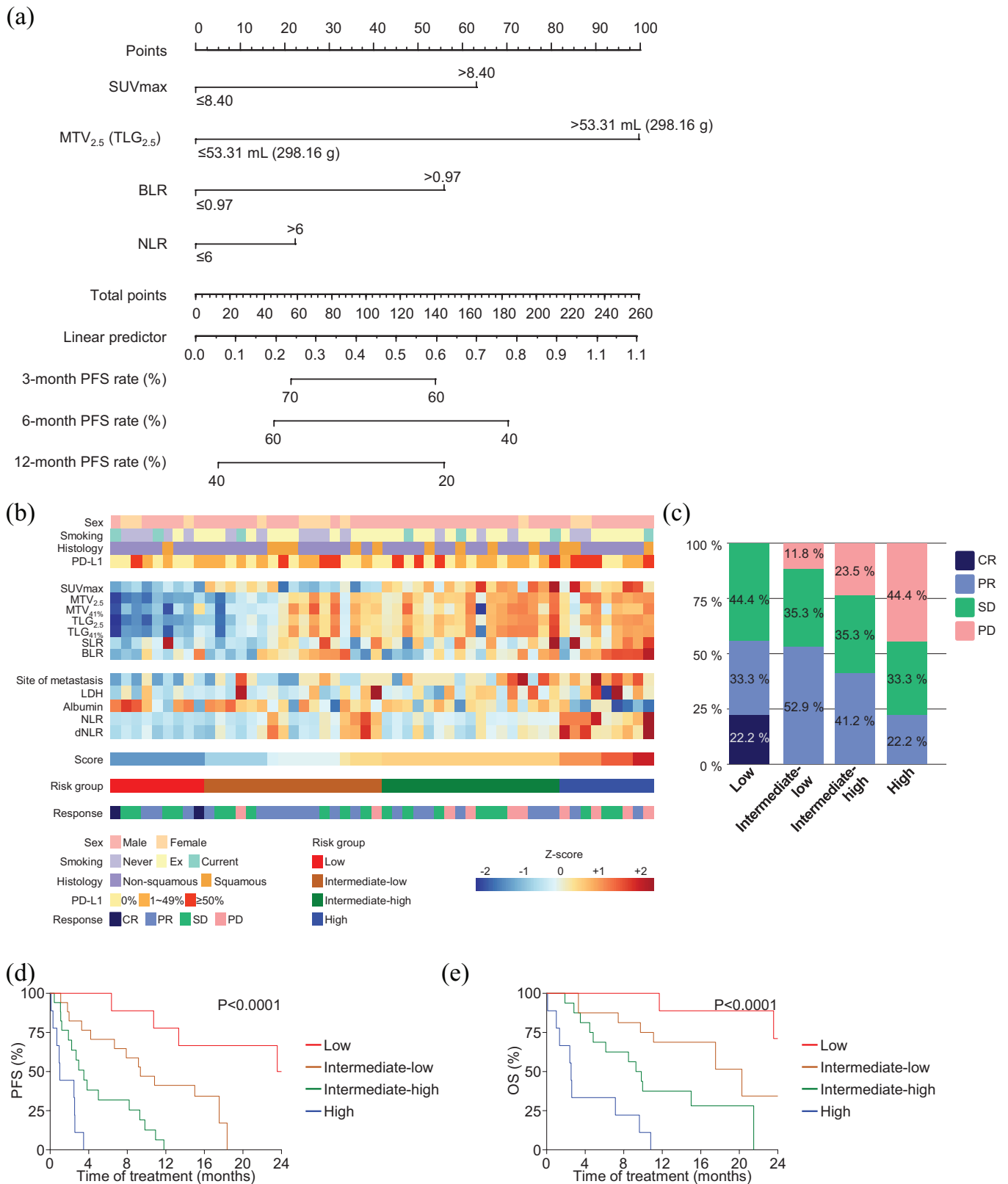
	Analysis for progression-free survival							
	Univariate		Multivariate		Multivariate		Multivariate	
	HR (95% CI)	p value	Step 1		Step 2		Step 3	
			HR (95% CI)	p value	HR (95% CI)	p value	HR (95% CI)	p value
SUVmax	3.548 (1.710–7.364)	0.001			2.974 (1.383–6.395)	0.005	2.855 (1.331–6.120)	0.007
MTV _{41%}	3.719 (1.943–7.119)	<0.001	1.890 (0.891–4.008)	0.097				
MTV _{2.5} ^a	5.135 (2.217–11.893)	<0.001	3.489 (1.305–9.325)	0.005	5.287 (2.225–12.560)	< 0.001	4.952 (1.847–13.277)	0.001
TLG _{41%}	3.610 (1.863–6.993)	<0.001	1.679 (0.750–3.737)	0.207				
TLG _{2.5} ^a	5.135 (2.217–11.893)	<0.001	3.582 (1.275–10.062)	0.015	5.287 (2.225–12.560)	< 0.001	4.952 (1.847–13.277)	0.001
SLR	2.312 (1.158–4.619)	0.018	2.124 (1.049–4.298)	0.036				
BLR	4.563 (1.811–11.494)	0.001	4.117 (1.604–10.568)	0.003	3.999 (1.503–10.635)	0.005	4.547 (1.655–12.488)	0.003
Sites of metastasis	2.747 (1.392–5.418)	0.004			2.278 (1.101–4.712)	0.026	1.405 (0.635–3.110)	0.402
LDH	2.595 (1.371–4.913)	0.003			1.809 (0.912–3.589)	0.090		
Albumin	0.991 (0.473–2.078)	0.981						
NLR	2.835 (1.329–6.047)	0.007			2.520 (1.150–5.520)	0.021	3.068 (1.386–6.793)	0.006
dNLR	2.248 (0.985–5.126)	0.054						

BLR, bone marrow-to-liver ratio of the SUV; CI, confidence interval; dNLR, derived NLR; HR, hazard ratio; LDH, lactate dehydrogenase; MTV, metabolic tumour volume; NLR, neutrophil-to-lymphocyte ratio; SLR, spleen-to-liver ratio of SUV; SUVmax, maximum standardized uptake value; TLG, total lesion glycolysis.

^aPatients' subgroup classified based on MTV_{2.5} and TLG_{2.5} is identical.

In this study, we analysed glycolysis index of the spleen, bone marrow, and liver besides that of the tumour to explore the significance of a systemic environment in predicting the outcome. Several studies revealed that ¹⁸F-FDG uptake in the spleen or bone marrow reflects the systemic inflammation in patients with infection or autoimmune disease.^{48,49} In patients with cancer, concurrent inflammation can be associated with increased ¹⁸F-FDG uptake in the spleen or bone marrow.⁵⁰ We found that measuring BLR can be useful as an independent predictive factor along

with tumour-intrinsic ¹⁸F-FDG uptake in patients receiving chemoimmunotherapy, highlighting the importance of systemic inflammation in dictating the treatment outcome of chemoimmunotherapy in NSCLC. Accordingly, both SLR and BLR were significantly correlated with NLR (Supplemental Figure 3), which have been recently suggested as biomarkers for systemic inflammation and unresponsiveness to ICB in patients with cancer.⁵¹ In addition, both BLR and NLR could independently predict patient outcomes in multivariate analysis, allowing a subtle



stratification of patients with NSCLC receiving chemoimmunotherapy. Up to now, predictive significance of inflammatory markers combined with PET/CT variables was investigated in NSCLC patients treated with first-line chemotherapy or immunotherapy.^{24,52,53} Continuing these efforts, our study is the first one to explore the predictive value of PET/CT parameters combined with clinicolaboratory variables in patients treated with chemoimmunotherapy to the best of our knowledge.

Given the heterogeneous response pattern and suboptimal response rate of NSCLC upon treatment with immune checkpoint inhibitors or chemotherapy, noninvasive methods can be useful for selecting the optimal treatment approach, predicting the outcome, and monitoring the response. In this regard, ¹⁸F-FDG PET/CT radiomics can be valuable sources to evaluate the metabolic properties of tumours, intra-tumoural heterogeneity, and systemic inflammation. Correspondingly, various attempts have been made to interrogate PET/CT radiomics with the genetic and immune landscapes of cancer, including those of NSCLC.^{54,55} These efforts have extended to devising treatment strategies and predicting individual patient prognosis using deep-learning models.^{45,56} Considering that biomarkers that can predict treatment response of chemoimmunotherapy in NSCLC have not been identified yet, our work may be the initial point to accelerate the utilization of PET/CT radiomics as biomarkers for pembrolizumab plus platinum-doublet chemotherapy.

The present study has a few limitations. First, the number of patients is relatively small and the analysis was retrospective in nature, warranting further validation in a prospective cohort with larger sample sizes. Second, performance status of the patients was not captured. Third, response evaluation was conducted based on RECIST 1.1 rather than iRECIST,⁵⁷ although pseudoprogression was not observed in the study populations. Fourth, the heterogeneous nature of the group of patients regarding histology, chemotherapeutic agents, and PD-L1 TPS might have confounding effects on the results. Fifth, the OS was relatively short compared to the updated results of KEYNOTE-189⁵⁸ and final results of KEYNOTE-407,⁵⁹ which reflects the patient outcomes in real-world setting, as well as relatively lower PD-L1 expression and less frequent smokers in our study cohort. Finally, the interval between the ¹⁸F-FDG PET/CT scan and the first

treatment was heterogeneous among patients, which might influence the results.

In summary, a prediction model that incorporated PET/CT parameters as well as clinicolaboratory variables was identified, and its predictive significance in patients with NSCLC receiving chemoimmunotherapy as a first-line treatment was proven. Our work establishes a framework for the noninvasive stratification of patients with distinct prognosis and guides optimal treatment options. Future studies are warranted to validate our findings in a prospective manner with a larger patient population.

Author contributions

Chang Gon Kim: Conceptualization; Data curation; Formal analysis; Funding acquisition; Investigation; Methodology; Software; Visualization; Writing – original draft

Sang Hyun Hwang: Conceptualization; Data curation; Formal analysis; Investigation; Methodology; Software; Visualization; Writing – original draft

Kyung Hwan Kim: Project administration; Resources; Writing – review & editing

Hong In Yoon: Project administration; Resources; Writing – review & editing

Hyo Sup Shim: Project administration; Resources; Writing – review & editing

Ji Hyun Lee: Project administration; Resources; Writing – review & editing

Yejeong Han: Project administration; Resources; Writing – review & editing

Beung-Chul Ahn: Project administration; Resources; Writing – review & editing

Min Hee Hong: Project administration; Resources; Writing – review & editing

Hye Ryun Kim: Project administration; Resources; Writing – review & editing

Byoung-Chul Cho: Project administration; Resources; Writing – review & editing

Arthur Cho: Conceptualization; Data curation; Formal analysis; Funding acquisition; Investigation; Methodology; Project administration; Resources; Software; Supervision; Writing – review & editing

Sun Min Lim: Conceptualization; Data curation; Formal analysis; Funding acquisition;

Investigation; Methodology; Project administration; Resources; Software; Supervision; Writing – review & editing

Conflict of interest statement

The authors declared no potential conflicts of interest with respect to the research, authorship, and/or publication of this article.

Funding

The authors disclosed receipt of the following financial support for the research, authorship, and/or publication of this article: This research was supported by the Basic Science Research Program through the National Research Foundation of Korea (NRF) funded by the Ministry of Education, Science and Technology (NRF-2016R1D1A1B01014677 to A.C. and NRF-2019R1A2C4069993 to S.M.L.) and Young Medical Scientist Research Grant Program of the Daewoong Foundation (DY20206 P to C.G.K.).

Supplemental material

Supplemental material for this article is available online.

References

- Herbst RS, Morgensztern D and Boshoff C. The biology and management of non-small cell lung cancer. *Nature* 2018; 553: 446–454.
- Wei SC, Duffy CR and Allison JP. Fundamental mechanisms of immune checkpoint blockade therapy. *Cancer Discov* 2018; 8: 1069–1086.
- Ribas A and Wolchok JD. Cancer immunotherapy using checkpoint blockade. *Science* 2018; 359: 1350–1355.
- Garon EB, Rizvi NA, Hui R, *et al.* Pembrolizumab for the treatment of non-small-cell lung cancer. *N Engl J Med* 2015; 372: 2018–2028.
- Reck M, Rodríguez-Abreu D, Robinson AG, *et al.* Pembrolizumab versus chemotherapy for PD-L1-positive non-small-cell lung cancer. *N Engl J Med* 2016; 375: 1823–1833.
- Paz-Ares L, Luft A, Vicente D, *et al.* Pembrolizumab plus chemotherapy for squamous non-small-cell lung cancer. *N Engl J Med* 2018; 379: 2040–2051.
- Hellmann MD, Paz-Ares L, Bernabe Caro R, *et al.* Nivolumab plus ipilimumab in advanced non-small-cell lung cancer. *N Engl J Med* 2019; 381: 2020–2031.
- Brahmer J, Reckamp KL, Baas P, *et al.* Nivolumab versus docetaxel in advanced squamous-cell non-small-cell lung cancer. *New Engl J Med* 2015; 373: 123–135.
- Borghaei H, Paz-Ares L, Horn L, *et al.* Nivolumab versus docetaxel in advanced nonsquamous non-small-cell lung cancer. *N Engl J Med* 2015; 373: 1627–1639.
- Gandhi L, Rodríguez-Abreu D, Gadgeel S, *et al.* Pembrolizumab plus chemotherapy in metastatic non-small-cell lung cancer. *N Engl J Med* 2018; 378: 2078–2092.
- Lim SM, Hong MH and Kim HR. Immunotherapy for non-small cell lung cancer: current landscape and future perspectives. *Immune Netw* 2020; 20: e10.
- Yu H, Boyle TA, Zhou C, *et al.* PD-L1 expression in lung cancer. *J Thorac Oncol* 2016; 11: 964–975.
- Rizvi H, Sanchez-Vega F, La K, *et al.* Molecular determinants of response to anti-programmed cell death (PD)-1 and anti-programmed death-ligand 1 (PD-L1) blockade in patients with non-small-cell lung cancer profiled with targeted next-generation sequencing. *J Clin Oncol* 2018; 36: 633–641.
- Sun R, Limkin EJ, Vakalopoulou M, *et al.* A radiomics approach to assess tumour-infiltrating CD8 cells and response to anti-PD-1 or anti-PD-L1 immunotherapy: an imaging biomarker, retrospective multicohort study. *Lancet Oncol* 2018; 19: 1180–1191.
- Rizvi NA, Hellmann MD, Snyder A, *et al.* Cancer immunology. Mutational landscape determines sensitivity to PD-1 blockade in non-small cell lung cancer. *Science* 2015; 348: 124–128.
- Hugo W, Zaretsky JM, Sun L, *et al.* Genomic and transcriptomic features of response to anti-PD-1 therapy in metastatic melanoma. *Cell* 2016; 165: 35–44.
- Chowell D, Morris LGT, Grigg CM, *et al.* Patient HLA class I genotype influences cancer response to checkpoint blockade immunotherapy. *Science* 2018; 359: 582–587.
- Sacher AG and Gandhi L. Biomarkers for the clinical use of PD-1/PD-L1 inhibitors in non-small-cell lung cancer: a review. *JAMA Oncol* 2016; 2: 1217–1222.
- Mok TSK, Wu YL, Kudaba I, *et al.* Pembrolizumab versus chemotherapy for previously untreated, PD-L1-expressing, locally

- advanced or metastatic non-small-cell lung cancer (KEYNOTE-042): a randomised, open-label, controlled, phase 3 trial. *Lancet* 2019; 393: 1819–1830.
20. Reck M, Rodríguez-Abreu D, Robinson AG, *et al.* Updated analysis of KEYNOTE-024: pembrolizumab versus platinum-based chemotherapy for advanced non-small-cell lung cancer with PD-L1 tumor proportion score of 50% or greater. *J Clin Oncol* 2019; 37: 537–546.
 21. Carbone DP, Reck M, Paz-Ares L, *et al.* First-line nivolumab in stage IV or recurrent non-small-cell lung cancer. *N Engl J Med* 2017; 376: 2415–2426.
 22. Aide N, Hicks RJ, Le Tourneau C, *et al.* FDG PET/CT for assessing tumour response to immunotherapy: report on the EANM symposium on immune modulation and recent review of the literature. *Eur J Nucl Med Mol Imaging* 2019; 46: 238–250.
 23. Mu W, Tunali I, Gray JE, *et al.* Radiomics of (18)F-FDG PET/CT images predicts clinical benefit of advanced NSCLC patients to checkpoint blockade immunotherapy. *Eur J Nucl Med Mol Imaging* 2020; 47: 1168–1182.
 24. Seban RD, Mezquita L, Berenbaum A, *et al.* Baseline metabolic tumor burden on FDG PET/CT scans predicts outcome in advanced NSCLC patients treated with immune checkpoint inhibitors. *Eur J Nucl Med Mol Imaging* 2020; 47: 1147–1157.
 25. Sharma A, Mohan A, Bhalla AS, *et al.* Role of various metabolic parameters derived from baseline 18F-FDG PET/CT as prognostic markers in non-small cell lung cancer patients undergoing platinum-based chemotherapy. *Clin Nucl Med* 2018; 43: e8–e17.
 26. Usmanij EA, Natroshvili T, Timmer-Bonte JNH, *et al.* The predictive value of early in-treatment (18)F-FDG PET/CT response to chemotherapy in combination with bevacizumab in advanced nonsquamous non-small cell lung cancer. *J Nucl Med* 2017; 58: 1243–1248.
 27. Lee JW, Seo KH, Kim ES, *et al.* The role of (18)F-fluorodeoxyglucose uptake of bone marrow on PET/CT in predicting clinical outcomes in non-small cell lung cancer patients treated with chemoradiotherapy. *Eur Radiol* 2017; 27: 1912–1921.
 28. Seban RD, Rouzier R, Latouche A, *et al.* Total metabolic tumor volume and spleen metabolism on baseline [18F]-FDG PET/CT as independent prognostic biomarkers of recurrence in resected breast cancer. *Eur J Nucl Med Mol Imaging* 2021; 48: 3560–3570.
 29. Seban RD, Robert C, Dercle L, *et al.* Increased bone marrow SUVmax on 18F-FDG PET is associated with higher pelvic treatment failure in patients with cervical cancer treated by chemoradiotherapy and brachytherapy. *Oncoimmunology* 2019; 8: e1574197.
 30. Lee JW, Choi JS, Lyu J, *et al.* Prognostic significance of (18)F-fluorodeoxyglucose uptake of bone marrow measured on positron emission tomography in patients with small cell lung cancer. *Lung Cancer* 2018; 118: 41–47.
 31. Gretten FR and Grivennikov SI. Inflammation and cancer: triggers, mechanisms, and consequences. *Immunity* 2019; 51: 27–41.
 32. Im HJ, Pak K, Cheon GJ, *et al.* Prognostic value of volumetric parameters of (18)F-FDG PET in non-small-cell lung cancer: a meta-analysis. *Eur J Nucl Med Mol Imaging* 2015; 42: 241–251.
 33. Boellaard R, Delgado-Bolton R, Oyen WJ, *et al.* FDG PET/CT: EANM procedure guidelines for tumour imaging: version 2.0. *Eur J Nucl Med Mol Imaging* 2015; 42: 328–354.
 34. Lee JW, Kim SY, Han SW, *et al.* [(18)F] FDG uptake of bone marrow on PET/CT for predicting distant recurrence in breast cancer patients after surgical resection. *EJNMMI Res* 2020; 10: 72.
 35. Ahn SS, Hwang SH, Jung SM, *et al.* Evaluation of spleen glucose metabolism using (18)F-FDG PET/CT in patients with febrile autoimmune disease. *J Nucl Med* 2017; 58: 507–513.
 36. Eisenhauer EA, Therasse P, Bogaerts J, *et al.* New response evaluation criteria in solid tumours: revised RECIST guideline (version 1.1). *Eur J Cancer* 2009; 45: 228–247.
 37. Bigot F, Castanon E, Baldini C, *et al.* Prospective validation of a prognostic score for patients in immunotherapy phase I trials: the Gustave Roussy Immune Score (GRIm-Score). *Eur J Cancer* 2017; 84: 212–218.
 38. Arkenau HT, Barriuso J, Olmos D, *et al.* Prospective validation of a prognostic score to improve patient selection for oncology phase I trials. *J Clin Oncol* 2009; 27: 2692–2696.
 39. Garrido-Laguna I, Janku F, Vaklavas C, *et al.* Validation of the Royal Marsden Hospital prognostic score in patients treated in the phase I Clinical Trials Program at the MD Anderson Cancer Center. *Cancer* 2012; 118: 1422–1428.
 40. Ettinger DS, Wood DE, Aisner DL, *et al.* NCCN guidelines insights: non-small cell lung cancer,

- version 2.2021. *J Natl Compr Canc Netw* 2021; 19: 254–266.
41. Wu YL, Planchard D, Lu S, *et al.* Pan-Asian adapted clinical practice guidelines for the management of patients with metastatic non-small-cell lung cancer: a CSCO-ESMO initiative endorsed by JSMO, KSMO, MOS, SSO and TOS. *Ann Oncol* 2019; 30: 171–210.
 42. Dall’Olio FG, Calabrò D, Conci N, *et al.* Baseline total metabolic tumour volume on 2-deoxy-2-[18F]fluoro-d-glucose positron emission tomography-computed tomography as a promising biomarker in patients with advanced non-small cell lung cancer treated with first-line pembrolizumab. *Eur J Cancer* 2021; 150: 99–107.
 43. Castello A, Rossi S, Mazziotti E, *et al.* Hyperprogressive disease in patients with non-small cell lung cancer treated with checkpoint inhibitors: the role of (18)F-FDG PET/CT. *J Nucl Med* 2020; 61: 821–826.
 44. Burger IA, Casanova R, Steiger S, *et al.* 18F-FDG PET/CT of non-small cell lung carcinoma under neoadjuvant chemotherapy: background-based adaptive-volume metrics outperform TLG and MTV in predicting histopathologic response. *J Nucl Med* 2016; 57: 849–854.
 45. Sun X, Xiao Z, Chen G, *et al.* A PET imaging approach for determining EGFR mutation status for improved lung cancer patient management. *Sci Transl Med* 2018; 10: eaan8840.
 46. Luan X, Huang Y, Gao S, *et al.* (18)F-alfatide PET/CT may predict short-term outcome of concurrent chemoradiotherapy in patients with advanced non-small cell lung cancer. *Eur J Nucl Med Mol Imaging* 2016; 43: 2336–2342.
 47. Mattonen SA, Davidzon GA, Benson J, *et al.* Bone marrow and tumor radiomics at (18)F-FDG PET/CT: impact on outcome prediction in non-small cell lung cancer. *Radiology* 2019; 293: 451–459.
 48. Pijl JP, Kwee TC, Slart R, *et al.* Clinical implications of increased uptake in bone marrow and spleen on FDG-PET in patients with bacteremia. *Eur J Nucl Med Mol Imaging* 2021; 48: 1467–1477.
 49. Carrasquillo JA, Chen CC, Price S, *et al.* 18F-FDG PET imaging features of patients with autoimmune lymphoproliferative syndrome. *Clin Nucl Med* 2019; 44: 949–955.
 50. Salaun PY, Gastinne T, Bodet-Milin C, *et al.* Analysis of ¹⁸F-FDG PET diffuse bone marrow uptake and splenic uptake in staging of Hodgkin’s lymphoma: a reflection of disease infiltration or just inflammation? *Eur J Nucl Med Mol Imaging* 2009; 36: 1813–1821.
 51. Kim CG, Kim C, Yoon SE, *et al.* Hyperprogressive disease during PD-1 blockade in patients with advanced hepatocellular carcinoma. *J Hepatol* 2021; 74: 350–359.
 52. Seban RD, Assié JB, Giroux-Leprieur E, *et al.* Prognostic value of inflammatory response biomarkers using peripheral blood and [18F]-FDG PET/CT in advanced NSCLC patients treated with first-line chemo- or immunotherapy. *Lung Cancer* 2021; 159: 45–55.
 53. Seban RD, Assié JB, Giroux-Leprieur E, *et al.* Association of the metabolic score using baseline FDG-PET/CT and dNLR with immunotherapy outcomes in advanced NSCLC patients treated with first-line pembrolizumab. *Cancers* 2020; 12: 2234.
 54. Zhang J, Zhao X, Zhao Y, *et al.* Value of pre-therapy (18)F-FDG PET/CT radiomics in predicting EGFR mutation status in patients with non-small cell lung cancer. *Eur J Nucl Med Mol Imaging* 2020; 47: 1137–1146.
 55. Lambin P, Leijenaar RTH, Deist TM, *et al.* Radiomics: the bridge between medical imaging and personalized medicine. *Nat Rev Clin Oncol* 2017; 14: 749–762.
 56. Mu W, Jiang L, Zhang J, *et al.* Non-invasive decision support for NSCLC treatment using PET/CT radiomics. *Nat Commun* 2020; 11: 5228.
 57. Seymour L, Bogaerts J, Perrone A, *et al.* IRECIST: guidelines for response criteria for use in trials testing immunotherapeutics. *Lancet Oncol* 2017; 18: e143–e152.
 58. Gadgeel S, Rodríguez-Abreu D, Speranza G, *et al.* Updated analysis from KEYNOTE-189: pembrolizumab or placebo plus pemetrexed and platinum for previously untreated metastatic nonsquamous non-small-cell lung cancer. *J Clin Oncol* 2020; 38: 1505–1517.
 59. Paz-Ares L, Vicente D, Tafreshi A, *et al.* A randomized, placebo-controlled trial of pembrolizumab plus chemotherapy in patients with metastatic squamous NSCLC: protocol-specified final analysis of KEYNOTE-407. *J Thorac Oncol* 2020; 15: 1657–1669.